Computer Aided Geometric Design 63 (2018) 122–134

Contents lists available at ScienceDirect

Computer Aided Geometric Design

www.elsevier.com/locate/cagd

Operation mode analysis of 3-RPS parallel manipulators based on their design parameters

Abhilash Nayak [a], Thomas Stigger [b], Manfred L. Husty [b], Philippe Wenger [c], Stéphane Caro [c,*]

[a] *École Centrale de Nantes, Laboratoire des Sciences du Numérique de Nantes (LS2N), 1 rue de la Noë, 44321 Nantes, France*
[b] *Unit Geometry and CAD, University of Innsbruck, Austria*
[c] *CNRS, Laboratoire des Sciences du Numérique de Nantes (LS2N), École Centrale de Nantes, 1 rue de la Noë, UMR CNRS 6004, 44321 Nantes, France*

ARTICLE INFO

Article history:
Available online 17 May 2018

Keywords:
Study's kinematic mapping
3-RPS
Parallel manipulator
Operation modes

ABSTRACT

It is known that a 3-RPS parallel manipulator with an equilateral triangle base and an equilateral triangle platform has two operation modes (Schadlbauer et al., 2014) whereas a 3-RPS cube manipulator with a cube shaped base and an equilateral triangle platform has only one operation mode (Nurahmi et al., 2014). This behavior is indeed a result of the difference in the architectures of these manipulators. Therefore, this paper deals with the operation mode analysis of 3-RPS parallel manipulators based on their design parameters. Study's kinematic mapping is exploited to derive the constraint equations of the manipulators under study. A linear combination of the constraint equations independent of the joint variables is compared with a general quadric in the 7-dimensional projective space $\mathbb{P}^7$ to obtain some relations between the design parameters of 3-RPS manipulators with coplanar revolute joints, such that those manipulators have two operation modes. Some special cases and a numerical example are considered to emphasize the proposed approach and highlight the contributions of the paper.

1. Introduction

The 3-RPS parallel manipulator is a three degree-of-freedom (DOF) spatial mechanism, initially proposed by Hunt (1983). This manipulator allows one pure vertical translation and two rotations about axes parallel to the horizontal plane, but since those axes do not remain fixed when the manipulator moves, the two rotations generate two parasitic horizontal translations. The mechanism is composed of three identical limbs connecting its base to its moving platform. Each limb consists of a revolute joint, a prismatic joint and a spherical joint mounted in series.

Several arrangements of the joints are possible, e.g. the R-joint axes in the base frame can be tangential to a circle, parallel or intersect at a common point.

Several research works have dealt with the kinematic analysis of the 3-RPS parallel manipulator. Huang and Fang (1995) described the constraints of the manipulator using screw theory. The number of solutions to the inverse kinematics was first published by Nanua et al. (1990) and Tsai (1999), Self-motions were investigated by Schadlbauer et al. (2013) in which

* Corresponding author.
E-mail addresses: abhilash.nayak@ls2n.fr (A. Nayak), thomas.stigger@uibk.ac.at (T. Stigger), manfred.husty@uibk.ac.at (M.L. Husty), philippe.wenger@ls2n.fr (P. Wenger), stephane.caro@ls2n.fr (S. Caro).

https://doi.org/10.1016/j.cagd.2018.05.003
0167-8396/

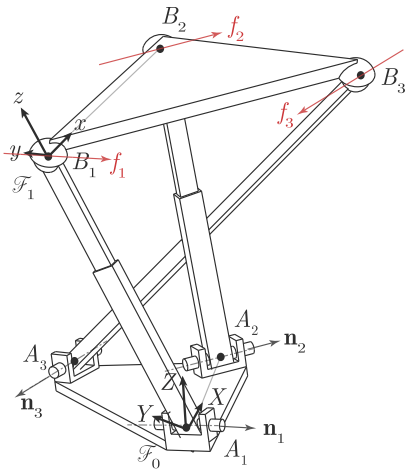

Fig. 1. Architecture of a 3-RPS parallel manipulator with coplanar revolute joints.

a spatial 3-RPS Manipulator was considered with R-joints tangential to the base circum-circle. Workspace and joint space analysis using quaternions was done by Chablat et al. (2014), and more special configurations of the 3-RPS manipulator like the 3-RPS cube manipulator as well as the synthesis of design parameters with respect to specific operation modes were both investigated by Nurahmi et al. (2014; 2015). Moreover, a complete algebraic analysis of the 3-RPS parallel manipulator was published, using Study's kinematic mapping in Schadlbauer et al. (2014) and in Schadlbauer et al. (2012). Gallardo et al. (2008) analyzed the kinematics of the 3-RPS parallel manipulator by using screw theory.

The motion capabilities of the 3-RPS parallel manipulator were exploited in telescope applications studied by Carretero et al. (1997) and in machine tool heads, investigated by Hernández et al. (2008).

The application for medical purposes like human machine interactions were investigated in Verde et al. (2009), including the control of the manipulator with PID controllers.

The subject of this paper is about the determination of some conditions on the design parameters of 3-RPS manipulators with coplanar revolute joint axes for those manipulators to have two operation modes.

The paper is organized as follows: Section 2 presents the architecture and parameterization of 3-RPS manipulators with coplanar revolute joint axes. Section 3 expresses their constraint equations as a function of Study parameters and independently of joint variables. Section 4 deals with the operation mode analysis of the manipulators under study and gives some conditions on their design parameters to lead to two operation modes. The operation modes of three 3-RPS parallel manipulators with coplanar revolute joints defined based on the foregoing conditions on design parameters are analyzed in Section 5 as illustrative examples. Some discussions and conclusions are given in Sec. 6.

2. Manipulator architectures

The investigated spatial parallel manipulator shown in Fig. 1 consists of a moving platform connected to a fixed base with three limbs. Each limb is composed of a revolute joint, a prismatic joint and a spherical joint mounted in series.[1] The three prismatic joints are actuated. Fig. 2 represents a RPS limb. The base of the 3-RPS manipulator is specified by 3 base-points A_1, A_2 and A_3 in the fixed frame $\mathscr{F}_0$. The fixed frame is defined such that A_1 is the origin of the coordinate frame, A_2 is along the x-axis and A_3 is an arbitrary point in the XY-plane. B_1, B_2 and B_3 are the vertices of the triangular moving-platform, B_1 is the origin of the moving-platform frame $\mathscr{F}_1$, B_2 is along the x-axis of $\mathscr{F}_1$ and B_3 lies in the xy-plane.

The ith revolute joint axis of direction $\mathbf{n}_i$ is perpendicular to the direction of the ith prismatic joint, namely,

$$\mathbf{n}_i \cdot \overrightarrow{A_i B_i} = 0, \quad i = 1, 2, 3 \tag{1}$$

3. Kinematic modeling

To derive the constraint equations of the 3-RPS parallel manipulators with coplanar revolute joint axes, the homogeneous coordinates of point A_i and vector $\mathbf{n}_i$ are firstly expressed in frame $\mathscr{F}_0$ while that of the point B_i are expressed in frame $\mathscr{F}_1$:

$$^0\mathbf{a}_1 = (1, 0, 0, 0), \quad ^0\mathbf{a}_2 = (1, a_{12}, 0, 0), \quad ^0\mathbf{a}_3 = (1, a_{13}, a_{23}, 0), \tag{2}$$

[1] A revolute, prismatic and a spherical joint are denoted by R, P and S respectively.

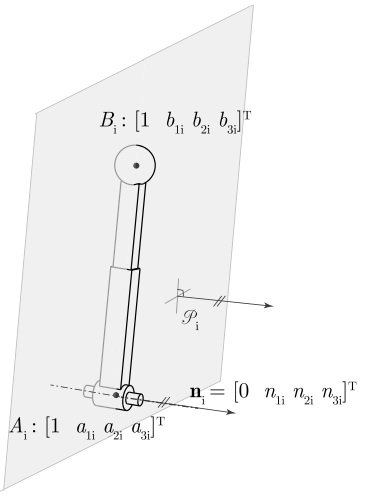

Fig. 2. A RPS limb.

$$^1\mathbf{b}_1 = (1,0,0,0), \quad ^1\mathbf{b}_2 = (1,b_{12},0,0), \quad ^1\mathbf{b}_3 = (1,b_{13},b_{23},0), \tag{3}$$

$$^0\mathbf{n}_1 = (0,n_{11},n_{21},n_{31}), \quad ^0\mathbf{n}_2 = (0,n_{12},n_{22},n_{32}), \quad ^0\mathbf{n}_3 = (0,n_{13},n_{23},n_{33}), \tag{4}$$

with the first entry of each vector being the homogenizing coordinate.[2] Since points B_i are given in the moving frame, a transformation is applied to obtain it in $\mathscr{F}_0$ frame. *Study's kinematic mapping* can be used for this purpose. It is a mapping from the special Euclidean motion group SE(3) to a seven-dimensional projective space $\mathbb{P}^7$ (Husty and Schröcker, 2013). The transformation to obtain $^0\mathbf{b}_i$ from $^1\mathbf{b}_i$ is given in Eq. (5)

$$^0\mathbf{T}_1 = \frac{1}{\Delta}\begin{bmatrix} \Delta & 0 & 0 & 0 \\ d_1 & x_0^2 + x_1^2 - x_2^2 - x_3^2 & -2x_0x_3 + 2x_1x_2 & 2x_0x_2 + 2x_1x_3 \\ d_2 & 2x_0x_3 + 2x_1x_2 & x_0^2 - x_1^2 + x_2^2 - x_3^2 & -2x_0x_1 + 2x_2x_3 \\ d_3 & -2x_0x_2 + 2x_1x_3 & 2x_0x_1 + 2x_2x_3 & x_0^2 - x_1^2 - x_2^2 + x_3^2 \end{bmatrix} \tag{5}$$

with $\Delta = x_0^2 + x_1^2 + x_2^2 + x_3^2 \neq 0$ and $d_1 = -2x_0y_1 + 2x_1y_0 - 2x_2y_3 + 2x_3y_2$, $d_2 = -2x_0y_2 + 2x_1y_3 + 2x_2y_0 - 2x_3y_1$, $d_3 = -2x_0y_3 - 2x_1y_2 + 2x_2y_1 + 2x_3y_0$, where x_j, y_j, $j = 0,1,2,3$ are the so called *Study parameters* of the transformation $^0\mathbf{T}_1$. A point $P = (x_0 : x_1 : x_2 : x_3 : y_0 : y_1 : y_2 : y_3) \in \mathbb{P}^7$ represents an Euclidean transformation, if and only if P lies in a 6-dimensional quadric, $S_6^2 \in \mathbb{P}^7$ called as the *Study quadric*:

$$S_6^2 : x_0y_0 + x_1y_1 + x_2y_2 + x_3y_3 = 0 \tag{6}$$

The geometric constraints of the parallel manipulator can be derived as follows. As the prismatic joints are actuated, the distance between points A_i and B_i is equal to the prismatic joint length r_i. Therefore, the following first three distance constraints arise:

$$g_i : (^0\mathbf{a}_i - ^0\mathbf{b}_i)^T(^0\mathbf{a}_i - ^0\mathbf{b}_i) - r_i^2 = 0, \quad i = 1,2,3. \tag{7}$$

The next three geometric constraints of the manipulator is derived from the perpendicularity between the revolute joint and the prismatic joint direction within each limb, namely, from Eq. (1):

$$g_{i+3} : {}^0\mathbf{n}_i^T(^0\mathbf{a}_i - ^0\mathbf{b}_i) = 0, \quad i = 1,2,3. \tag{8}$$

As a result, the six constraint equations are expressed as follows after some mathematical simplifications:

$$g_1 := \left(x_0^2 + x_1^2 + x_2^2 + x_3^2\right) r_1^2 - 4y_0^2 - 4y_1^2 - 4y_2^2 - 4y_3^2 = 0 \tag{9a}$$

$$\begin{aligned} g_2 := {} & \left(x_0^2 + x_1^2 + x_2^2 + x_3^2\right)(r_2^2 - b_{12}^2 - a_{12}^2) + \left(2x_0^2 + 2x_1^2 - 2x_2^2 - 2x_3^2\right)a_{12}b_{12} \\ & + (-4x_0y_1 + 4x_1y_0 - 4x_2y_3 + 4x_3y_2)a_{12} + (4x_0y_1 - 4x_1y_0 - 4x_2y_3 + 4x_3y_2)b_{12} \end{aligned}$$

[2] A vector expressed in $\mathscr{F}_0$ is denoted as $^0\{\cdot\}$ whereas a vector expressed in $\mathscr{F}_1$ is indicated as $^1\{\cdot\}$.

$$-4y_0^2-4y_1^2-4y_2^2-4y_3^2=0 \tag{9b}$$

$$\begin{aligned}g_3 :=& \left(x_0^2+x_1^2+x_2^2+x_3^2\right)(r_3^2-a_{13}^2-a_{23}^2-b_{13}^2-b_{23}^2)+\left(2x_0^2+2x_1^2-2x_2^2-2x_3^2\right)a_{13}b_{13}\\&+(-4x_0x_3+4x_1x_2)a_{13}b_{23}+(-4x_0y_1+4x_1y_0-4x_2y_3+4x_3y_2)a_{13}+(4x_0x_3+4x_1x_2)a_{23}b_{13}\\&+\left(2x_0^2-2x_1^2+2x_2^2-2x_3^2\right)a_{23}b_{23}+(-4x_0y_2+4x_1y_3+4x_2y_0-4x_3y_1)a_{23}\\&+(4x_0y_1-4x_1y_0-4x_2y_3+4x_3y_2)b_{13}+(4x_0y_2+4x_1y_3-4x_2y_0-4x_3y_1)b_{23}\\&-4y_0^2-4y_1^2-4y_2^2-4y_3^2=0\end{aligned} \tag{9c}$$

$$g_4 := (2x_0y_1-2x_1y_0+2x_2y_3-2x_3y_2)n_{11}+(2x_0y_2-2x_1y_3-2x_2y_0+2x_3y_1)n_{21}=0 \tag{9d}$$

$$\begin{aligned}g_5 :=& (2x_0y_1-2x_1y_0+2x_2y_3-2x_3y_2)n_{12}+(2x_0y_2-2x_1y_3-2x_2y_0+2x_3y_1)n_{22}\\&+a_{12}n_{12}\left(x_0^2+x_1^2+x_2^2+x_3^2\right)+\left(-x_0^2-x_1^2+x_2^2+x_3^2\right)b_{12}n_{12}\\&+(-2x_0x_3-2x_1x_2)b_{12}n_{22}=0\end{aligned} \tag{9e}$$

$$\begin{aligned}g_6 :=& (2x_0y_1-2x_1y_0+2x_2y_3-2x_3y_2)n_{13}+(2x_0y_2-2x_1y_3-2x_2y_0+2x_3y_1)n_{23}\\&-(a_{13}n_{13}+a_{23}n_{23})\left(x_0^2+x_1^2+x_2^2+x_3^2\right)+\left(-x_0^2-x_1^2+x_2^2+x_3^2\right)b_{13}n_{13}\\&+\left(-x_0^2+x_1^2-x_2^2+x_3^2\right)b_{23}n_{23}+(-2x_0x_3-2x_1x_2)b_{13}n_{23}+(2x_0x_3-2x_1x_2)b_{23}n_{13}=0\end{aligned} \tag{9f}$$

It should be noted that those six equations are a function of fifteen design parameters a_{12}, a_{13}, a_{23}, b_{12}, b_{13}, b_{23}, n_{ij} ($i, j \in \{1,2,3\}$), three actuated prismatic joint variables r_1, r_2, r_3 and the Study parameters.

4. Operation modes

This section aims to find the conditions on the fifteen design parameters such that the 3-RPS manipulator with coplanar revolute joints can exhibit more than one operation mode. Since the R-joint axes are assumed coplanar, $n_{31}=n_{32}=n_{33}=0$.

From the standpoint of algebraic geometry, it is known that the existence of more than one operation mode requires the factorization of a polynomial belonging to the ideal of constraint polynomials (preferably the ones independent of actuated joint variables) (Schadlbauer et al., 2014). In this context, an ideal $\mathcal{I}$ is considered such that it is a subset of the field of Study parameters:

$$\mathcal{I}=\langle g_4, g_5, g_6\rangle \mid \mathcal{I}\subseteq K[x_0,x_1,x_2,x_3,y_0,y_1,y_2,y_3] \tag{10}$$

From the definition of an ideal, if a polynomial $g\in\mathcal{I}$ and $h\in K$, K being the field over which the ideal $\mathcal{I}$ is defined, then $hg\in\mathcal{I}$ (Cox et al., 2007). From Eqs. (9) and (10), a polynomial g is defined such that

$$g=h_1g_4+h_2g_5+h_3g_6\in\mathcal{I},\ \text{where } h_i\neq 0\in K[x_0,x_1,x_2,x_3,y_0,y_1,y_2,y_3],\ i=1,2,3 \tag{11}$$

For simplicity, h_i is only allowed to be a function of design parameters. This assumption forces the polynomial g to be quadratic. To this end, the problem boils down to find the coefficients h_i such that g can be factorized. In search of linear factors, two general linear equations are introduced in Eq. (12) and are multiplied to obtain a general quadratic polynomial s_{12} in the kinematic image space, $\mathbb{P}^7$.

$$\begin{aligned}&s_1 : m_1x_0+m_2x_1+m_3x_2+m_4x_3+m_5y_0+m_6y_1+m_7y_2+m_8y_3=0\\&s_2 : n_1x_0+n_2x_1+n_3x_2+n_4x_3+n_5y_0+n_6y_1+n_7y_2+n_8y_3=0\\&s_{12}=s_1\cdot s_2\end{aligned} \tag{12}$$

where m_k and n_k, $k=1,\ldots,8$ are constants. Equating the respective coefficients of g and s_{12} leads to a system of 36 linear equations in 31 unknowns. Solving for all the parameters b_{12}, b_{13}, b_{23}, a_{12}, a_{13}, a_{23}, h_1, h_2, h_3, $m_k, n_k, k=1,\ldots,8$, yields 36 solutions. It is noteworthy that some equations are dependent and the system is underdetermined. Nonetheless, the *solve* function in Maple parametrizes the solutions in terms of one or more unknowns. Investigating the solution set reveals that there are some trivial solutions (complex ones and the ones with $h_i=0$, $a_{12}=0$, $a_{13}=0$, $a_{23}=0$, $b_{12}=0$, $b_{13}=0$ or $b_{23}=0$) and some are special cases of the general one ($n_{ij}=0$, $i=1,2$, $j=1,2,3$). The focus is on the two general solutions:

Solution 1

$$m_1=\frac{\left(n_{13}\pm\sqrt{n_{13}^2+n_{23}^2}\right)m_4}{n_{23}},\ m_2=0,\ m_3=0,\ m_4=m_4,\ m_5=0,\ m_6=0,\ m_7=0,\ m_8=0, \tag{13a}$$

$$n_1 = \frac{2\left(n_{13} \pm \sqrt{{n_{13}}^2 + {n_{23}}^2}\right) b_{23} h_3}{m_4},\ n_2 = 0,\ n_3 = 0,\ n_4 = 2\,\frac{b_{23} h_3 n_{23}}{m_4},\ n_5 = 0,\ n_6 = 0,\ n_7 = 0,\ n_8 = 0, \tag{13b}$$

$$a_{12} = \frac{(n_{11}n_{22} - n_{12}n_{21})\,(a_{13}n_{13} + a_{23}n_{23})}{(n_{11}n_{23} - n_{13}n_{21})\,n_{12}},\ a_{13} = a_{13}, a_{23} = a_{23} \tag{13c}$$

$$b_{12} = -\frac{b_{23}\left({n_{13}}^2 + {n_{23}}^2\right)(n_{11}n_{22} - n_{12}n_{21})}{(n_{12}n_{23} - n_{13}n_{22})\,(n_{11}n_{23} - n_{13}n_{21})},\ b_{13} = -\frac{b_{23}\,(n_{12}n_{13} + n_{22}n_{23})}{n_{12}n_{23} - n_{13}n_{22}},\ b_{23} = b_{23} \tag{13d}$$

$$h_1 = \frac{h_3\,(n_{12}n_{23} - n_{13}n_{22})}{n_{11}n_{22} - n_{12}n_{21}},\ h_2 = -\frac{h_3\,(n_{11}n_{23} - n_{13}n_{21})}{n_{11}n_{22} - n_{12}n_{21}},\ h_3 = h_3 \tag{13e}$$

Solution 2

$$m_1 = 0,\ m_2 = \frac{\left(n_{13} \pm \sqrt{{n_{13}}^2 + {n_{23}}^2}\right) m_3}{n_{23}},\ m_3 = m_3,\ m_4 = 0,\ m_5 = 0,\ m_6 = 0,\ m_7 = 0,\ m_8 = 0, \tag{14a}$$

$$n_1 = 0,\ n_2 = \frac{2 b_{23} h_3 {n_{23}}^2}{\left(n_{13} \pm \sqrt{{n_{13}}^2 + {n_{23}}^2}\right) m_3},\ n_3 = -2\,\frac{b_{23} h_3 n_{23}}{m_3},\ n_4 = 0,\ n_5 = 0,\ n_6 = 0,\ n_7 = 0,\ n_8 = 0, \tag{14b}$$

$$a_{12} = \frac{(n_{11}n_{22} - n_{12}n_{21})\,(a_{13}n_{13} + a_{23}n_{23})}{(n_{11}n_{23} - n_{13}n_{21})\,n_{12}},\ a_{13} = a_{13}, a_{23} = a_{23} \tag{14c}$$

$$b_{12} = \frac{b_{23}\left({n_{13}}^2 + {n_{23}}^2\right)(n_{11}n_{22} - n_{12}n_{21})}{(n_{12}n_{23} - n_{13}n_{22})\,(n_{11}n_{23} - n_{13}n_{21})},\ b_{13} = \frac{b_{23}\,(n_{12}n_{13} + n_{22}n_{23})}{n_{12}n_{23} - n_{13}n_{22}},\ b_{23} = b_{23} \tag{14d}$$

$$h_1 = \frac{h_3\,(n_{12}n_{23} - n_{13}n_{22})}{n_{11}n_{22} - n_{12}n_{21}},\ h_2 = -\frac{h_3\,(n_{11}n_{23} - n_{13}n_{21})}{n_{11}n_{22} - n_{12}n_{21}},\ h_3 = h_3 \tag{14e}$$

Upon substitution of Solution 1 into Eq. (11) or Eq. (12) that describe the general quadric, the following conic comes out:

$$s_{12} = g = 2\,b_{23} h_3 \left(2\,n_{13} x_0 x_3 - n_{23} {x_0}^2 + n_{23} {x_3}^2\right) \tag{15}$$

The conic is degenerate and can be factorized as follows:

$$s_{12} = g = 2\,\frac{b_{23} h_3}{n_{23}} \left(x_3 \sqrt{{n_{13}}^2 + {n_{23}}^2} + n_{13} x_3 - n_{23} x_0\right) \left(x_3 \sqrt{{n_{13}}^2 + {n_{23}}^2} - n_{13} x_3 + n_{23} x_0\right),\ n_{23} \neq 0 \tag{16}$$

$$= -2 b_{23}\, h_3\, n_{23} \left(x_0 - x_3 \left(\sqrt{\hat{n}^2 + 1} + \hat{n}\right)\right) \left(x_0 + x_3 \left(\sqrt{\hat{n}^2 + 1} - \hat{n}\right)\right),\ \hat{n} = \frac{n_{13}}{n_{23}},\ n_{23} \neq 0, \tag{17}$$

bringing to light two operation modes characterized by:

$$\begin{aligned} &\text{Operation mode 1}: x_0 - x_3 \left(\sqrt{\hat{n}^2 + 1} + \hat{n}\right) = 0 \\ &\text{Operation mode 2}: x_0 + x_3 \left(\sqrt{\hat{n}^2 + 1} - \hat{n}\right) = 0, \quad \hat{n} = \frac{n_{13}}{n_{23}},\ n_{23} \neq 0. \end{aligned} \tag{18}$$

In the same vein, upon substituting Solution 2 into Eq. (11) or Eq. (12) results in the general quadric

$$s_{12} = g = -2 \left(2\,n_{13} x_1 x_2 - n_{23} {x_1}^2 + n_{23} {x_2}^2\right) b_{23} h_3, \tag{19}$$

which splits into two polynomials characterizing the following two operation modes:

$$\begin{aligned} &\text{Operation mode 1}: x_1 - x_2 \left(\sqrt{\hat{n}^2 + 1} + \hat{n}\right) = 0 \\ &\text{Operation mode 2}: x_1 + x_2 \left(\sqrt{\hat{n}^2 + 1} - \hat{n}\right) = 0, \quad \hat{n} = \frac{n_{13}}{n_{23}},\ n_{23} \neq 0 \end{aligned} \tag{20}$$

As a result, when the design parameters b_{12}, b_{13} and b_{23} follow the ratio

$$\begin{aligned} b_{12} : b_{13} : b_{23} = {} & (n_{11}n_{22} - n_{12}n_{21}) \left({n_{13}}^2 + {n_{23}}^2\right) \\ & : (n_{12}n_{13} + n_{22}n_{23})\,(-n_{13} n_{21} + n_{11} n_{23}) \\ & : \pm\,(-n_{13} n_{22} + n_{12} n_{23})\,(-n_{13} n_{21} + n_{11} n_{23}), \end{aligned} \tag{21}$$

and parameters a_{12}, a_{13} and a_{23} satisfy the relation

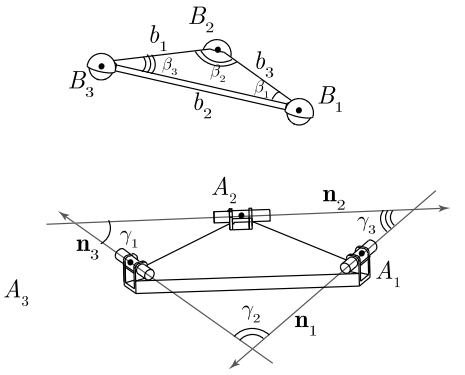

Fig. 3. Similarity condition between the moving platform triangle and the triangle enclosed by the R-joint axes.

$$(n_{11}n_{23} - n_{13}n_{21})\, a_{12}n_{12} + (n_{12}n_{21} - n_{11}n_{22})\, (+a_{13}n_{13} + a_{23}n_{23}) = 0, \tag{22}$$

then, the 3-RPS parallel manipulator with coplanar revolute joint axes has two operation modes characterized by Eqs. (18) or (20). To derive these characteristic polynomials starting from the plane constraints, the scalar coefficients of their linear combination must follow the ratio

$$h_1 : h_2 : h_3 = n_{12}n_{23} - n_{13}n_{22} :\ n_{11}n_{23} - n_{13}n_{21} :\ n_{11}n_{22} - n_{12}n_{21}. \tag{23}$$

The condition in Eq. (21) can be geometrically interpreted as the similarity (also called as homothety) between the moving platform triangle and the triangle enclosed by the three R-joint axes. This claim is proven as follows. Fig. 3 shows the moving platform triangle and the triangle enclosed by the revolute joints. The sides of the moving platform triangle are $b_1 = \sqrt{(b_{13} - b_{12})^2 + b_{23}^2}$, $b_2 = |b_{13} - b_{12}|$ and $b_3 = |b_{12}|$. Knowing the sides, the cosine of the angles β_1, β_2 and β_3 can be determined using the cosine rule. Similarly, the cosine of the angles γ_1, γ_2 and γ_3 between the R-joint axes $\mathbf{n}_1$, $\mathbf{n}_2$ and $\mathbf{n}_3$, can be determined. Equating the cosine of respective angles results in three equations.[3]

$$\cos(\beta_i) = \cos(\gamma_i) \implies \frac{b_j^2 + b_k^2 - b_i^2}{2b_j b_k} = \frac{\mathbf{n}_j \mathbf{n}_k}{||\mathbf{n}_j||||\mathbf{n}_k||} \quad i, j, k = (123) \tag{24}$$

Solving the equations for b_{12}, b_{13} and b_{23} yields the conditions in Eq. (21) proving that the considered triangles are similar (or homothetic).

Besides, Eq. (22) has a geometrical meaning too. It can be written as the determinant of a matrix, $\mathbf{P}$:

$$|\mathbf{P}| = \begin{vmatrix} n_{11} & n_{21} & 0 \\ n_{12} & n_{22} & -n_{12}a_{12} \\ n_{13} & n_{23} & -n_{13}a_{13} - n_{23}a_{23} \end{vmatrix} = 0 \tag{25}$$

$|\mathbf{P}|$ is the Grassmannian of three lines $\mathscr{L}_1$, $\mathscr{L}_2$ and $\mathscr{L}_3$ which are the projections of planes $\mathscr{P}_1$, $\mathscr{P}_2$ and $\mathscr{P}_3$ onto the XY-plane as shown in Fig. 4. The equation of a line $\mathscr{L}_i, i = 1, 2, 3$, orthogonal to R-joint axis $\mathbf{n}_i$ and passing through a point A_i is $n_{1i}x_0 + n_{2i}y_0 - \mathbf{n}_i^T \mathbf{a}_i,\ i = 1, 2, 3$. Therefore, $|\mathbf{P}| = 0$ implies that lines $\mathscr{L}_i$ are concurrent, namely, planes $\mathscr{P}_1$, $\mathscr{P}_2$ and $\mathscr{P}_3$ intersect at line $\mathscr{M}$.

Thus, a 3-RPS parallel manipulator with coplanar revolute joint axes will have two operation modes if the following geometric conditions are satisfied

i Moving platform triangle is homothetic to the triangle enclosed by the revolute joint axes.
ii The three planes normal to the three revolute joint axes, respectively, have a common line of intersection.

It can be shown that the above conditions are also necessary for the existence of two operation modes as explained thereafter.

Equations (18) and (20) are the polynomials characterizing the two operation modes. The transition between them is when both polynomials vanish at the same time, i.e., when $x_0 = x_3 = 0$ for Solution 1 and when $x_1 = x_2 = 0$ for Solution 2. Transition pose is known to be a constraint singularity and in case of Solution 1, it corresponds to configurations in which the moving platform is upside down as explained in Schadlbauer et al. (2014; 2012). For Solution 2, the transition pose

[3] The notation (1,2,3) represents a cyclic permutation. It means that i, j, k are initially assigned to values 1,2,3, respectively, 2,3,1, subsequently and 3,1,2, finally.

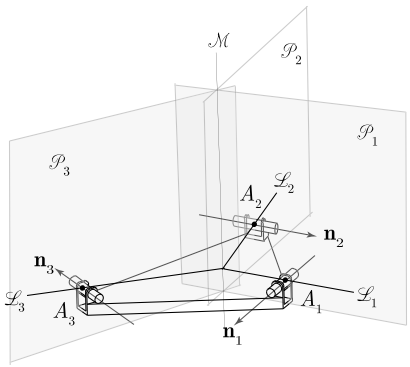

Fig. 4. The planes normal to R-joint axes must have a common line of intersection.

corresponds to configurations in which the moving platform is in an upright position parallel to the fixed base. The existence of two operation modes definitely implies a constraint singularity that separates those operation modes but the reciprocity is not necessarily true as explained in subsection 5.2. This fact is exploited to prove the necessary conditions for a 3-RPS PM to have two operation modes.

According to screw theory, it is well known that a parallel manipulator reaches a constraint singularity when its constraint wrench system is rank deficient (Zlatanov et al., 2002; Amine et al., 2017). At this instant, the PM gains at least one dof. The constraint wrench system of a 3-RPS PM shown in Fig. 1 is spanned by three forces f_1, f_2 and f_3 that are parallel to the revolute joint axes $\mathbf{n}_1, \mathbf{n}_2$ and $\mathbf{n}_3$ and pass through points B_1, B_2 and B_3, respectively. A constraint singularity implies that variety spanned by these three lines has a rank lower than 3. This can happen only when these lines reduce to a planar pencil of lines, i.e., when they are coplanar and concurrent. The Plücker coordinates of the force lines can be written as follows:

$$\mathbf{f}_1 = [{}^0\mathbf{n}_1,\ {}^0\mathbf{b}_1 \times {}^0\mathbf{n}_1] \tag{26a}$$

$$\mathbf{f}_2 = [{}^0\mathbf{n}_2,\ {}^0\mathbf{b}_2 \times {}^0\mathbf{n}_2] \tag{26b}$$

$$\mathbf{f}_3 = [{}^0\mathbf{n}_3,\ {}^0\mathbf{b}_3 \times {}^0\mathbf{n}_3] \tag{26c}$$

Coplanarity condition

Any two lines intersect when the reciprocal product of their Plücker coordinates vanishes. Therefore, the coplanarity condition can be formulated as the mutual vanishing of the reciprocal product between the force lines yielding the following three equations:

$$E_1 := 2\,\frac{b_{12}\,(x_0x_2 - x_1x_3)\,(n_{11}n_{22} - n_{12}n_{21})}{{x_0}^2 + {x_1}^2 + {x_2}^2 + {x_3}^2} = 0 \tag{27a}$$

$$E_2 := 2\,\frac{(n_{11}n_{23} - n_{13}n_{21})\,(b_{13}x_0x_2 - b_{13}x_1x_3 - b_{23}x_0x_1 - b_{23}x_2x_3)}{{x_0}^2 + {x_1}^2 + {x_2}^2 + {x_3}^2} = 0 \tag{27b}$$

$$E_3 : -2\,\frac{(n_{12}n_{23} - n_{13}n_{22})\,(b_{12}x_0x_2 - b_{12}x_1x_3 - b_{13}x_0x_2 + b_{13}x_1x_3 + b_{23}x_0x_1 + b_{23}x_2x_3)}{{x_0}^2 + {x_1}^2 + {x_2}^2 + {x_3}^2} = 0 \tag{27c}$$

Solving the previous system of equations in Eq. (27) for Study parameters x_0, x_1, x_2, x_3 gives two solutions:

$$x_0 = x_3 = 0, \tag{28}$$

$$x_1 = x_2 = 0. \tag{29}$$

Calculating ${}^0\mathbf{b}_i$, $i = 1, 2, 3$ with solutions (28) or (29) shows that the z-coordinates of the resulting points are the same proving that they indeed lie in a plane parallel to the XY-plane.

Concurrency condition

Case 1: $x_0 = x_3 = 0$

The z-coordinate of points B_i is expressed $\dfrac{-2(x_1y_2 - x_2y_1)}{x_1^2 + x_2^2}$. Without loss of generality, these lines can now be projected to the XY-plane to simplify the concurrency condition. Their projections have the equations:

$$L_i := -n_{2i}X + n_{1i}Y - (-n_{2i}\,{}^0b_{ix} + n_{1i}\,{}^0b_{iy}) = 0,\ i = 1, 2, 3, \tag{30}$$

where ${}^0b_{iy}$ and ${}^0b_{iy}$ are the x- and y-coordinates of point B_i, respectively. Therefore, the condition for concurrency of the three lines defined by equations $L_i = 0$ is

$$
\begin{vmatrix} -n_{21} & n_{11} & n_{21}{}^0b_{1x} - n_{11}{}^0b_{1y} \\ -n_{22} & n_{12} & n_{22}{}^0b_{2x} - n_{12}{}^0b_{2y} \\ -n_{23} & n_{13} & n_{23}{}^0b_{3x} - n_{13}{}^0b_{3y} \end{vmatrix}
$$

$$
\begin{aligned}
&= (b_{12}n_{11}n_{22}n_{23} - b_{12}n_{13}n_{21}n_{22} - b_{13}n_{11}n_{22}n_{23} + b_{13}n_{12}n_{21}n_{23} - b_{23}n_{11}n_{13}n_{22} + b_{23}n_{12}n_{13}n_{21})(x_2^2 - x_1^2) \\
&\quad + 2(b_{12}n_{11}n_{12}n_{23} - b_{12}n_{12}n_{13}n_{21} - b_{13}n_{11}n_{13}n_{22} + b_{13}n_{12}n_{13}n_{21} + b_{23}n_{11}n_{22}n_{23} - b_{23}n_{12}n_{21}n_{23})x_1x_2 \\
&= 0
\end{aligned} \tag{31}
$$

Equating the coefficients to zero leads to the following relations between the design parameters:

$$
b_{12} = -\frac{(n_{11}n_{22} - n_{12}n_{21})\, b_{23}\left({n_{13}}^2 + {n_{23}}^2\right)}{(-n_{13}\, n_{22} + n_{12}n_{23})\,(-n_{13}\, n_{21} + n_{11}n_{23})}, \quad b_{13} = -\frac{(n_{12}n_{13} + n_{22}n_{23})\, b_{23}}{n_{12}n_{23} - n_{13}n_{22}}, \quad b_{23} = b_{23} \tag{32}
$$

which are exactly those defined by Eq. (13d).

Furthermore, upon substitution of the values of b_{12} and b_{13} and $x_0 = x_3 = 0$ in constraint equations $g_1 = g_2 = g_3 = 0$ defined by Eqs. (9d)–(9f) and eliminating b_{23}, results in the following equation:

$$
(n_{11}n_{23} - n_{13}n_{21})\, a_{12}n_{12} + (n_{12}n_{21} - n_{11}n_{22})\,(+a_{13}n_{13} + a_{23}n_{23}) = 0, \tag{33}
$$

which is the relation derived in Eq. (22).

Case 2: $x_1 = x_2 = 0$

In this case, we obtain the following symmetric relations between the design parameters:

$$
b_{12} = \frac{(n_{11}n_{22} - n_{12}n_{21})\, b_{23}\left({n_{13}}^2 + {n_{23}}^2\right)}{(-n_{13}\, n_{22} + n_{12}n_{23})\,(-n_{13}\, n_{21} + n_{11}n_{23})}, \quad b_{13} = \frac{(n_{12}n_{13} + n_{22}n_{23})\, b_{23}}{n_{12}n_{23} - n_{13}n_{22}}, \quad b_{23} = b_{23}, \tag{34}
$$

$$
(n_{11}n_{23} - n_{13}n_{21})\, a_{12}n_{12} + (n_{12}n_{21} - n_{11}n_{22})\,(+a_{13}n_{13} + a_{23}n_{23}) = 0, \tag{35}
$$

that corresponds to the relations derived in Eqs. (14d) and (22), respectively.

As a conclusion, the following theorem can be stated:

Theorem 1. *A 3-RPS parallel manipulator with coplanar revolute joint axes will have two operation modes if and only if the following geometric conditions are satisfied*

i *Moving platform triangle is homothetic to the triangle enclosed by the revolute joint axes.*
ii *The three planes normal to the three revolute joint axes, respectively, have a common line of intersection.*

Since the relationship between the number of operation modes and architecture is established, the design parameters can be chosen in such a way that a constraint singularity is avoided.

In case the revolute joint axes are no longer coplanar, equating a general quadric in $\mathbb{P}^7$ defined in Eq. (12) with the linear combination of the plane constraint polynomials g_4, g_5 and g_6 shown in Eqs. (9d)–(9f), does not yield any solution. The problem of finding the influence of design parameters on the operation modes of a general 3-RPS parallel manipulator is left for future work.

5. Examples

In this section, some example 3-RPS manipulators are considered to verify the proposed conditions.

5.1. Example 1: 3-RPS parallel manipulator with $n_{23} = 0$

The well-known 3-RPS parallel manipulator introduced by Hunt (1983) has been the spotlight of numerous research topics and applications (Huang and Fang, 1995, Schadlbauer et al., 2013, 2014, 2012, Chablat et al., 2014; Nurahmi et al., 2014; Gallardo et al., 2008; Verde et al., 2009). Its architecture is shown in Fig. 5. The moving platform and the base are equilateral triangles with circum-radius b and a, respectively. The R-joint axes are coplanar and tangential to the base circum-circle. The P-joint in each leg is normal to its corresponding R-joint axis. The design parameters are listed below:

$$
a_{12} = \sqrt{3}a, \quad a_{13} = \frac{\sqrt{3}}{2}a, \quad a_{23} = \frac{3}{2}a,
$$

$$
b_{12} = \sqrt{3}b, \quad b_{13} = \frac{\sqrt{3}}{2}b, \quad b_{23} = \frac{3}{2}b,
$$

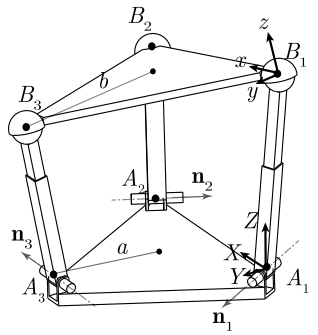

Fig. 5. A 3-RPS parallel manipulator with $n_{23} = 0$.

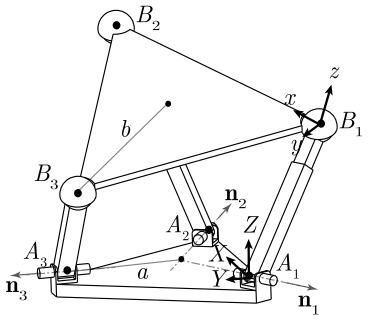

Fig. 6. A 3-RPS parallel manipulator with $n_{13} = 0$.

$$n_{11} = \frac{1}{2}, \quad n_{21} = -\frac{\sqrt{3}}{2}, \quad n_{31} = 0, \quad n_{12} = \frac{1}{2}, \quad n_{22} = \frac{\sqrt{3}}{2}, \quad n_{32} = 0, \quad n_{13} = -1, \quad n_{23} = 0, \quad n_{33} = 0. \tag{36}$$

Calculating the right hand side of Eq. (21) gives $b_{12} : b_{13} : b_{23} = \frac{\sqrt{3}}{2} : \frac{\sqrt{3}}{4} : \pm\frac{3}{4}$, which is consistent with the design parameters listed in Eq. (36). It is also straightforward to see that the design parameters satisfy Eq. (22). Thus, according to Theorem 1, the manipulator must exhibit two operation modes. To determine the characteristic equations of the operation modes, the plane constraint equations corresponding to Eq. (8) are considered:

$$g_4 := -\sqrt{3}x_0y_2 + \sqrt{3}x_1y_3 + \sqrt{3}x_2y_0 - \sqrt{3}x_3y_1 + x_0y_1 - x_1y_0 + x_2y_3 - x_3y_2 = 0 \tag{37}$$

$$\begin{aligned} g_5 :=& \sqrt{3}x_0y_2 - \sqrt{3}x_1y_3 - \sqrt{3}x_2y_0 + \sqrt{3}x_3y_1 + x_0y_1 - x_1y_0 + x_2y_3 - x_3y_2 + \frac{\sqrt{3}}{2}(x_0{}^2 + x_1{}^2 + x_2{}^2 \\ &+ x_3{}^2)a - \frac{\sqrt{3}}{2}(2\sqrt{3}x_0x_3 + 2\sqrt{3}x_1x_2 + x_0{}^2 + x_1{}^2 - x_2{}^2 - x_3{}^2)b = 0 \end{aligned} \tag{38}$$

$$\begin{aligned} g_6 :=& -2x_0y_1 + 2x_1y_0 - 2x_2y_3 + 2x_3y_2 - \frac{\sqrt{3}}{2}(x_0{}^2 + x_1{}^2 + x_2{}^2 + x_3{}^2)a - \frac{\sqrt{3}}{2}(2\sqrt{3}x_0x_3 - 2\sqrt{3}x_1x_2 \\ &- x_0{}^2 - x_1{}^2 + x_2{}^2 + x_3{}^2)b = 0. \end{aligned} \tag{39}$$

Equation (23) can be used to find the constants h_1, h_2 in terms of h_3 to be multiplied to the constraint polynomials g_4, g_5 and g_6, respectively to obtain a factorable polynomial g. For this manipulator, the design parameters yield $h_1 = h_3$ and $h_2 = h_3$. Thus from Eqs. (11) and (37)

$$g = h_1g_4 + h_2g_5 + h_3g_6 = h_3(g_4 + g_5 + g_6) = -6h_3bx_0x_3 \tag{40}$$

showing that the manipulator at hand can have two operation modes characterized by $x_0 = 0$ and $x_3 = 0$ as already presented in Schadlbauer et al. (2014; 2012). In fact, substituting $n_{23} = 0$ in Eq. (15) results in the factorable polynomial x_0x_3.

5.2. Example 2: 3-RPS parallel manipulator with $n_{13} = 0$

Another special case of the 3-RPS parallel manipulator is when the R-joint axes are intersecting as shown in Fig. 6. The base and the platform are still equilateral triangles with circum-radius a and b, respectively. Also, the P-joints are orthogonal to their corresponding R-joint axes in each leg. The design parameters for this manipulator are listed below:

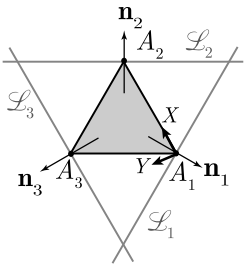

(a) $a_{12} = \sqrt{3}a, \quad a_{13} = \frac{\sqrt{3}}{2}a, \quad a_{23} = \frac{3}{2}a$

One operation mode

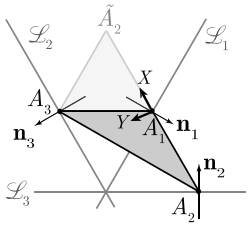

(b) $a_{12} = -\sqrt{3}a, \quad a_{13} = \frac{\sqrt{3}}{2}a, \quad a_{23} = \frac{3}{2}a$

Two operation modes

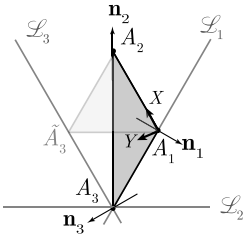

(c) $a_{12} = \sqrt{3}a, \quad a_{13} = -\frac{\sqrt{3}}{2}a, \quad a_{23} = \frac{3}{2}a$

Two operation modes

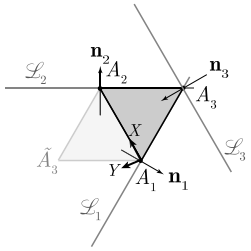

(d) $a_{12} = \sqrt{3}a, \quad a_{13} = \frac{\sqrt{3}}{2}a, \quad a_{23} = -\frac{3}{2}a$

Two operation modes

Fig. 7. Slight modification of design parameters can influence the number of operation modes.

$$
\begin{aligned}
&a_{12} = \sqrt{3}a, \quad a_{13} = \frac{\sqrt{3}}{2}a, \quad a_{23} = \frac{3}{2}a,\\
&b_{12} = \sqrt{3}b, \quad b_{13} = \frac{\sqrt{3}}{2}b, \quad b_{23} = \frac{3}{2}b,\\
&n_{11} = \frac{\sqrt{3}}{2}, \quad n_{21} = \frac{1}{2}, \quad n_{31} = 0, \quad n_{12} = \frac{\sqrt{3}}{2}, \quad n_{22} = -\frac{1}{2}, \quad n_{32} = 0, \quad n_{13} = 0, \quad n_{23} = 1, \quad n_{33} = 0
\end{aligned} \tag{41}
$$

The ratio between b_{12}, b_{13} and b_{23} calculated using Eq. (21) gives $b_{12} : b_{13} : b_{23} = -\frac{\sqrt{3}}{2} : -\frac{\sqrt{3}}{4} : \pm\frac{3}{4}$, which is consistent with the design parameters listed in Eq. (41). Thus, the condition i. of Theorem 1 is satisfied. It can also be verified by the fact that the R-joint axes intersect in a point, which is homothetic with the moving platform equilateral triangle. On the other hand, the left hand side of Eq. (22) gives $\frac{-3\sqrt{3}a}{2} \neq 0$ proving that this manipulator can have only one operation mode.[4] As a matter of fact, inspecting Fig. 6 reveals that the planes normal to $\mathbf{n}_i$ and passing through A_i do not have a common line of intersection and hence this manipulator cannot exhibit more than one operation mode since condition ii. of Theorem 1 is not satisfied. Fig. 7a shows the projections of planes $\mathscr{P}_i$ as lines $\mathscr{L}_i$ onto the XY-plane.

Nonetheless, the design parameters can be altered so that the condition ii. is satisfied. Changing $n_{ij}, i = 1, 2, j = 1, 2, 3$ might alter condition i. of Theorem 1, hence a_{12}, a_{13} or a_{23} can be changed so that condition i. is kept intact. From Eq. (22), writing a_{12} as a function of other design parameters and substituting the values from Eq. (41) yields $a_{12} = -\sqrt{3}a$. The design with $a_{12} = -\sqrt{3}a$ is shown in Fig. 7b and it exhibits two operation modes. $\tilde{A}_2$ represents the initial position of point A_2. In fact, a_{13} or a_{23} can also be changed similarly to obtain the designs shown in Figs. 7c and 7d, respectively. In these figures, $\tilde{A}_3$ represents the initial position of point A_3. Calculating $h_i, i = 1, 2, 3$ from Eq. (23) and substituting in the general quadric of Eq. (11) gives the characteristic polynomial of each operation mode as $x_0 - x_3$ and $x_0 + x_3$.

Consequently, it provides an interesting example of how architecture of a manipulator influences its number of operation modes. The procedure explained can be used to design 3-RPS parallel manipulators to have the necessary number of operation modes. Moreover, for a 3-RPS parallel manipulator with two operation modes, the constraint singularity between the operation modes can be escaped by slightly modifying the design parameters such that one of the conditions in Theorem 1 is not fulfilled.

[4] When $a = b$, the manipulator at hand can have a constraint singularity when the moving platform is parallel to the fixed base. However, it has only one operation mode. This is because, for a general 3-RPS PM, the variety of its constraint singularity condition is a surface whereas in this case it is reduced to a line parallel to the Z-axis and passing through the intersection of the R-joint axes. It is an interesting case of a constraint singularity that does not bifurcate the workspace into multiple operation modes.

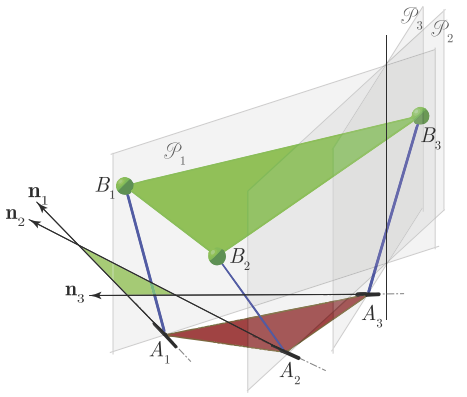

Fig. 8. A 3-RPS parallel manipulator with two operation modes characterized by $x_0 - x_3(2+\sqrt{5}) = 0$ and $x_0 - x_3(2-\sqrt{5}) = 0$.

5.3. Example 3: arbitrary design parameters

Finally, a numerical example is studied with the following arbitrary design parameters:

$$\begin{aligned} &a_{13} = 2, \quad a_{23} = 2, \quad b_{23} = 3, \\ &n_{11} = -3, \quad n_{21} = 5, \quad n_{31} = 0, \quad n_{12} = -3, \quad n_{22} = 2, \quad n_{32} = 0, \quad n_{13} = 2, \quad n_{23} = 1, \quad n_{33} = 0 \end{aligned} \tag{42}$$

The remaining design parameters a_{12}, b_{12} and b_{13} are calculated from the relations in Eqs. (22) and (21) so that the manipulator has two operation modes. Thus, $a_{12} = \dfrac{18}{13}$, $b_{12} = \pm\dfrac{135}{91}$ and $b_{13} = \pm\dfrac{12}{7}$. Fig. 8 shows the architecture of the manipulator at hand, where it can be pointed out that condition i. and ii. of Theorem 1 are satisfied. Substituting the design parameters with $b_{12} = -\dfrac{135}{91}$ and $b_{13} = -\dfrac{12}{7}$ in Eq. (16) gives

$$g := (x_0 - x_3(2+\sqrt{5}))(x_0 - x_3(2-\sqrt{5})) = 0 \tag{43}$$

whereas, substituting the design parameters with $b_{12} = \dfrac{135}{91}$ and $b_{13} = \dfrac{12}{7}$ in Eq. (16) gives

$$g := (x_1 - x_2(2+\sqrt{5}))(x_1 - x_2(2-\sqrt{5})) = 0 \tag{44}$$

The two polynomials $x_0 - x_3(2+\sqrt{5})$ and $x_0 - x_3(2-\sqrt{5})$ or $x_1 - x_2(2+\sqrt{5})$ and $x_1 - x_2(2-\sqrt{5})$ represent the two operation modes of the mechanism.[5]

Assuming the prismatic joints are actuated, the direct kinematics of the manipulator can be solved by substituting arbitrary values to joint parameters $r_1 = 2, r_2 = 2$ and $r_3 = 3$. The constraint equations $g_1 = 0$ to $g_6 = 0$ and $S_6^2 = 0$ can be written from Eqs. (6) and (9). Adding a normalization equation $x_0^2 + x_1^2 + x_2^2 + x_3^2 = 1$ (so that $\Delta \neq 0$ in Eq. (5)) yields a set of eight equations to be solved for eight Study parameters. Finding the Groebner basis of the ideal of constraint polynomials with a pure lexicographic monomial ordering $x_0 <_{lex} x_1 <_{lex} x_2 <_{lex} x_3 <_{lex} y_0 <_{lex} y_1 <_{lex} y_2 <_{lex} y_3$ results in a 16 degree univariate polynomial in variable y_3. As anticipated, the polynomial can be factorized into two polynomials of degree 8 each corresponding to the two operation modes. It shows that a 3-RPS parallel manipulator can have at most 8 solutions to its direct kinematics in each operation mode. When the joint parameters are fixed, the direct kinematics of a 3-RPS parallel manipulator amounts to locating three points on three fixed circles with centers A_i and radii r_i. To this end, a corollary follows as a consequence of Theorem 1:

Corollary 2. *For the 3-points on 3-circles problem, if the geometry satisfies the following conditions*

i *normals to the planes containing the circles and passing through their centers are coplanar,*
ii *planes containing the circles have a common line of intersection and*
iii *the triangle formed by the three points is homothetic to the triangle enclosed by three normals to the planes passing through the centers of the circles,*

then the 16 degree univariate characteristic polynomial factorizes into two 8 degree polynomials.

[5] To be able to factorize the polynomial g, the field of rational numbers must be extended to include $\sqrt{n_{23}^2 + n_{13}^2}$ i.e. $\sqrt{5}$ for this example.

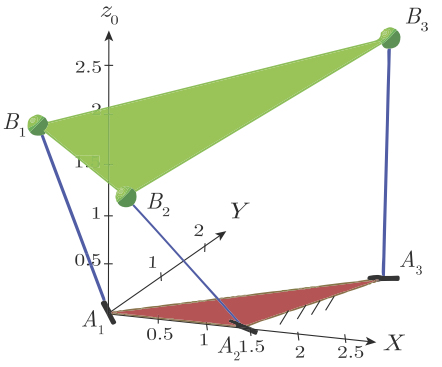

(a) $x_0 = 0.0593$, $x_1 = -0.2925$, $x_2 = -0.9206$, $x_3 = -0.2515$, $y_0 = 0.0001$, $y_1 = -0.8954$, $y_2 = 0.3571$, $y_3 = -0.2658$ OR
$x_0 = .9206$, $x_1 = .2515$, $x_2 = 0.0593$, $x_3 = -.2925$, $y_0 = -.3571$, $y_1 = .2658$, $y_2 = 0.0001$, $y_3 = -.8954$.

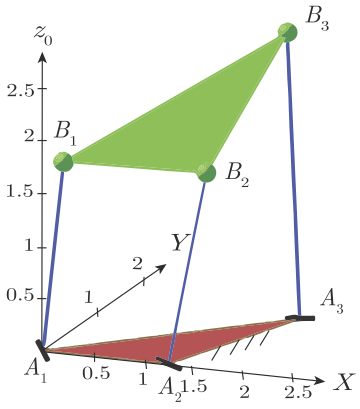

(b) $x_0 = 0.0264$, $x_1 = 0.0940$, $x_2 = -0.9889$, $x_3 = -0.1119$, $y_0 = -0.1607$, $y_1 = -0.9782$, $y_2 = -0.1060$, $y_3 = 0.0775$ OR
$x_0 = -.9889$, $x_1 = -.1119$, $x_2 = -0.0264$, $x_3 = -0.0940$, $y_0 = -.1060$, $y_1 = 0.0775$, $y_2 = .1607$, $y_3 = .9782$.

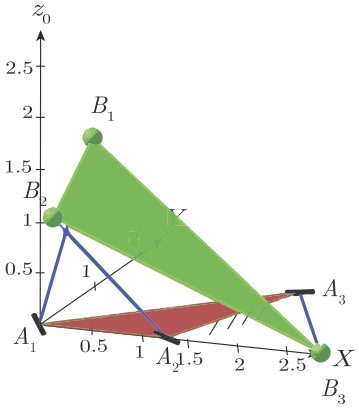

(c) $x_0 = 0.2482$, $x_1 = -0.6214$, $x_2 = -0.7407$, $x_3 = 0.0586$, $y_0 = -0.2019$, $y_1 = -0.7792$, $y_2 = 0.5742$, $y_3 = -0.1490$ OR
$x_0 = .7407$, $x_1 = -0.0586$, $x_2 = .2482$, $x_3 = -.6214$, $y_0 = -.5742$, $y_1 = .1490$, $y_2 = -.2019$, $y_3 = -.7792$.

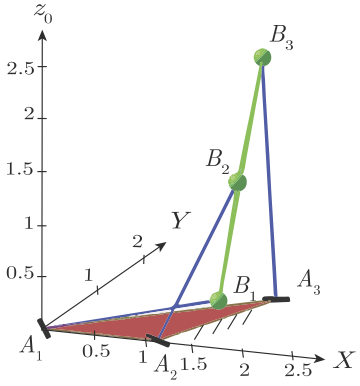

(d) $x_0 = -0.6304$, $x_1 = 0.0743$, $x_2 = -0.7582$, $x_3 = -0.1488$, $y_0 = -0.3408$, $y_1 = 0.5290$, $y_2 = 0.1872$, $y_3 = 0.7541$ OR
$x_0 = .7582$, $x_1 = .1488$, $x_2 = -.6304$, $x_3 = 0.0743$, $y_0 = -.1872$, $y_1 = -.7541$, $y_2 = -.3408$, $y_3 = .5290$.

Fig. 9. Solutions to direct kinematics of a 3-RPS manipulator with arbitrary design parameters.

For the above-mentioned example, eight real solutions to its direct kinematics problem are found. The solutions form four pairs of manipulator postures, one being the mirror image of another about the XY-plane. Four of these solutions are displayed in Fig. 9.

The first two solutions satisfy $\frac{x_0}{x_3} = 2 - \sqrt{5}$ or $\frac{x_1}{x_2} = 2 + \sqrt{5}$ and hence belong to the operation mode corresponding to $x_0 - x_3(2 - \sqrt{5}) = 0$ or $x_1 - x_2(2 + \sqrt{5}) = 0$, respectively while the last two satisfy $\frac{x_0}{x_3} = 2 + \sqrt{5}$ or $\frac{x_1}{x_2} = 2 - \sqrt{5}$ and hence belong to the operation mode characterized by $x_0 - x_3(2 + \sqrt{5}) = 0$ or $x_1 - x_2(2 - \sqrt{5}) = 0$.

6. Conclusions and future work

The influence of design parameters on the number of operation modes of a 3-RPS parallel manipulator with coplanar revolute joints was studied in this paper. The constraint equations of a general 3-RPS parallel manipulator were derived.

The linear combination of plane constraint polynomials were equated to a general quadric in $\mathbb{P}^7$ and the coefficients were solved to obtain two solutions with some relations between design parameters. These relations were substituted back into the general quadric and it factorized into two polynomials characterizing two operation modes. The conditions on the design parameters for the existence of two operation modes in 3-RPS manipulator with coplanar revolute joints was summarized as a theorem with proof. The first condition is the homothety between the moving platform triangle and the triangle enclosed by revolute joint axes, while the second condition is when three planes on which the spherical joints are confined to move have a common line of intersection. Two special cases were considered: one that has two operation modes and the other one with one operation mode. For the latter manipulator, it was shown that one can modify the design parameters to be able to have two operation modes. Finally, a numerical example was considered following the proposed theorem. Its characteristic 16 degree univariate polynomial is derived to show that it splits into two polynomials of degree 8 each, representing two operation modes. The direct kinematic solutions lying in each operation mode were shown.

Future work will include the influence of architecture on the operation modes of a 3-RPS parallel manipulator with non-coplanar revolute joints. Additionally, the proposed methodology will be extended to different parallel manipulators.

References

Amine, S., Mokhiamar, O., Caro, S., 2017. Classification of 3T1R parallel manipulators based on their wrench graph. J. Mech. Robot. 9 (1), 011003.

Carretero, J., Nahon, M., Gosselin, C., Buckham, B., 1997. Kinematic analysis of a three-dof parallel mechanism for telescope applications. In: Proceedings of the 1997 ASME Design Engineering Technical Conferences.

Chablat, D., Jha, R., Rouillier, F., Moroz, G., 2014. Workspace and joint space analysis of the 3-RPS parallel robot. In: ASME 2013 International Design Engineering Technical Conferences and Computers and Information in Engineering Conference, vol. 5A, pp. 1–10.

Cox, D.A., Little, J., O'Shea, D., 2007. Ideals, Varieties, and Algorithms: An Introduction to Computational Algebraic Geometry and Commutative Algebra, 3rd ed.. Undergrad. Texts Math.. Springer-Verlag New York, Inc., Secaucus, NJ, USA.

Gallardo, J., Orozco, H., Rico, J.M., 2008. Kinematics of 3-RPS parallel manipulators by means of screw theory. Int. J. Adv. Manuf. Technol. 36 (5), 598–605. https://doi.org/10.1007/s00170-006-0851-5.

Hernández, A., Altuzarra, O., Pinto, C., Amezua, E., 2008. Transitions in the velocity pattern of lower mobility parallel manipulators. Mech. Mach. Theory 43, 738–753.

Huang, Z., Fang, Y., 1995. Motion characteristics and rotational axis analysis of three dof parallel robot mechanisms. In: IEEE International Conference on Systems, Man and Cybernetics. Intelligent Systems for the 21st Century. Vancouver, BC, Canada, Oct. 22–25, 1995, pp. 67–71.

Hunt, K.H., 1983. Structural kinematics of in-parallel-actuated robot-arms. 105 (4), 705–712. https://doi.org/10.1115/1.3258540.

Husty, M.L., Schröcker, H.P., 2013. 21st Century Kinematics. Ch. Kinematics and Algebraic Geometry. Springer-Verlag London, London, pp. 85–123.

Nanua, P., Waldron, K.J., Murthy, V., 1990. Direct kinematic solution of a stewart platform. IEEE Trans. Robot. Autom. 6 (4), 438–444. https://doi.org/10.1109/70.59354.

Nurahmi, L., Schadlbauer, J., Husty, M., Wenger, P., Caro, S., 2014. Kinematic analysis of the 3-RPS cube parallel manipulator. In: 38th Mechanisms and Robotics Conference, vol. 5B.

Nurahmi, L., Caro, S., Wenger, P., 2015. Design of 3-RPS parallel manipulators based on operation modes. In: Proceedings of the 14th IFTOMM World Congress. October 25–30, 2015, Taipei, Taiwan.

Schadlbauer, J., Walter, D., Husty, M., 2012. A complete analysis of the 3-RPS parallel manipulator. In: Machines and Mechanisms. Narosa Publishing House, New Delhi, India, pp. 410–419.

Schadlbauer, J., Husty, M., Caro, S., Wenger, P., 2013. Self-motions of 3-RPS manipulators. Front. Mech. Eng. 8 (1), 62–69.

Schadlbauer, J., Walter, D., Husty, M., 2014. The 3-RPS parallel manipulator from an algebraic viewpoint. Mech. Mach. Theory 75 (Supplement C), 161–176. https://doi.org/10.1016/j.mechmachtheory.2013.12.007. http://www.sciencedirect.com/science/article/pii/S0094114X13002504.

Tsai, L.-W., 1999. Robot Analysis. John Wiley and Sons, Inc.

Verde, D., Stan, S.D., Manic, M., Balan, R., Matie, V., 2009. Kinematics analysis, workspace, design and control of 3-RPS and triglide medical parallel robots. In: 2009 2nd Conference on Human System Interactions, pp. 103–108.

Zlatanov, D., Bonev, I.A., Gosselin, C.M., 2002. Constraint singularities of parallel mechanisms. In: 2002 IEEE International Conference on Robotics and Automation (ICRA'02), vol. 1. IEEE, pp. 496–502.